研　究　速　報

UDC 539.375.5：539.431.3
669.384
620.186.4：620.187

Fatigue Cracks under Plane Stress in Electrodeposited Copper Single Crystal — Part Ⅲ

平面応力下における電着銅単結晶の疲れき裂（3）

Yoshiaki HAGIUDA* and Masahisa MATUNAGA*

萩生田　善明・松　永　正　久

1. Introduction

In previous reports[1], the authors discussed the uniformly distributed cracks on copper single crystal film deposited on plastics, and reported that many types of cracks were formed on {001} surface and that a crack formation process, was proposed by observing the initiation of cracks. In this report, types of cracks formed on {110} and {111} surfaces will be reported.

2. Experimental method

Copper single crystals were electrodeposited on plastics as previously reported[1]. Fatigue tests were performed by the same machine for reported bending, frequency was 210 cpm, strain amplitude $\varepsilon_a = 1.1 \times 10^{-3} \sim 1.5 \times 10^{-3}$, number of repetitions $N = 1 \times 10^5 \sim 1 \times 10^6$, unless otherwise stated.

3. Experimental results on {110} surface

Stress axis tested with {110} surface were <110>, <211> and <111>. Table 1 shows the values of

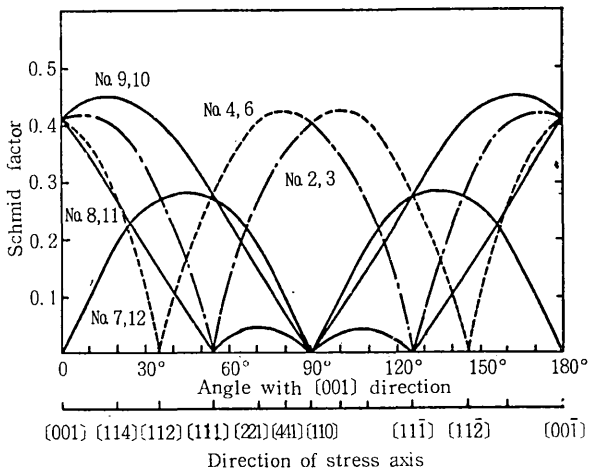

Fig. 1 Values of Schmid factor on (1$\bar{1}$0) plane

Table 1 Schmid factor of slip system on single crystal (1$\bar{1}$0) surface

Cross line with (111) surface (Crack direction)	Slip system			Stress axis						
	Slip plane	Slip direction	No	[001]	[114]	[112]	[111]	[221]	[441]	[110]
[11$\bar{2}$]	(111)	[1$\bar{1}$0]	1	0	0	0	0	0	0	0
		[01$\bar{1}$]	2	0.408	0.408	0.272	0	0.227	0.333	0.408
		[10$\bar{1}$]	3	0.408	0.408	0.272	0	0.227	0.333	0.408
[112]	(11$\bar{1}$)	[101]	4	0.408	0.227	0	0.272	0.408	0.433	0.408
		[1$\bar{1}$0]	5	0	0	0	0	0	0	0
		[011]	6	0.408	0.227	0	0.272	0.408	0.433	0.408
[110]	(1$\bar{1}$1)	[110]	7	0	0.182	0.272	0.272	0.182	0.098	0
		[10$\bar{1}$]	8	0.408	0.272	0.136	0	0.045	0.037	0
		[011]	9	0.408	0.454	0.408	0.272	0.136	0.062	0
	($\bar{1}$11)	[101]	10	0.408	0.454	0.408	0.272	0.136	0.062	0
		[01$\bar{1}$]	11	0.408	0.272	0.136	0	0.045	0.037	0
		[110]	12	0	0.182	0.272	0.272	0.182	0.098	0

Schmid facter in respect to slip plane, slip direction and stress axis on (1$\bar{1}$0) surface, and Fig. 1 shows the relationship, Fig. 2 illustrates crystal planes,

* Dept. of Mechanical Engineering and Naval Architecture, Institute of Industrial Science, Univ. of Tokyo.

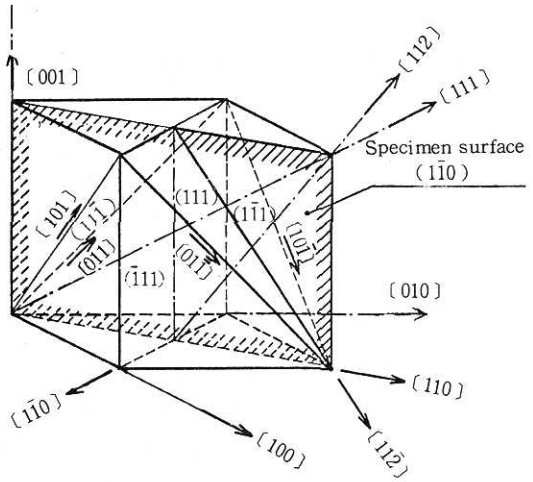

Fig. 2 Crystallographic representation on (1$\bar{1}$0) plane. slip planes and slip directions in fcc. The slip planes are (111), (11$\bar{1}$), (1$\bar{1}$1) and ($\bar{1}$11). The cracks appeared along [112], [11$\bar{2}$] and [110] orientations which are the crossing lines between (1$\bar{1}$0) surface and the slip planes.

(1) **[110] stress axis**

Symmetrical cracks were easily formed in [110] stress axis. The direction of cracks were along [112] and [11$\bar{2}$] which are cross lines of (1$\bar{1}$0) surface and (111), (11$\bar{1}$) slip planes. These directions formed 54° 44′ with stress axis and cross angle between these cracks was 70° 32′. Fig. 3 shows a typical crack pattern of this kind at strain amplitude $\varepsilon_a = 1.2 \times 10^{-3}$, $N = 1 \times 10^5$. Fig. 4 shows an electron-micrograph of the same speciments. This figure indicates clearly that fatigue slips in the order of 300 Å in distance appeared on whole surface and that the

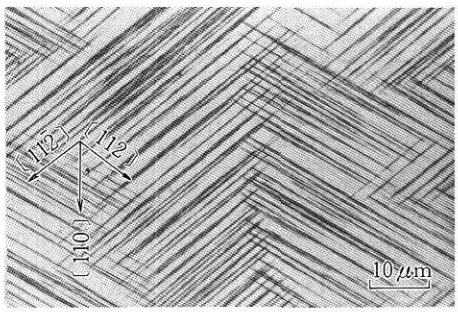

Fig. 3 Figure of crack on (1$\bar{1}$0) plane and [110] stress axis, $\varepsilon_a = 1.2 \times 10^{-3}$, $N = 1 \times 10^5$

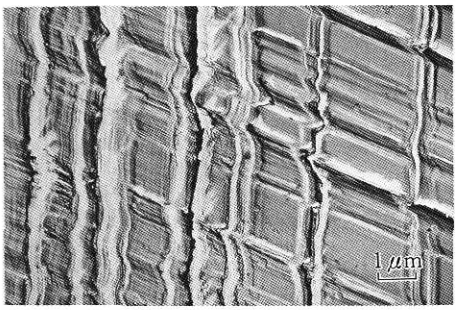

Fig. 4 Electron-micrograph of the same crack as Fig. 3. $\varepsilon_a = 1.2 \times 10^{-3}$, $N = 1 \times 10^5$

crackes were formed along the slip lines. An example of the minimum repetition was $N = 1 \times 10^5$ for $\varepsilon_a = 0.69 \times 10^{-3}$.

(2) **[001] stress axis**

Since values of Schmid factor are the same as that of the case in [110] stress axis and eight slip systems might be activated, it was anticipated that three directions of cracks along those of [112], [11$\bar{2}$] and [110] would be formed. Contrary to the anticipation, few slip lines could be obserbed, and no crack was formed at strain amplitude $\varepsilon_a = 1.38 \times 10^{-3}$ and $N = 3 \times 10^6$. Which are larger values than these of [110] stress axis. Fig. 5 shows an optical micrograph of the fatigued surface and this shows a different appearance in compared with other micrographs. This consists of boundaries and dence slip lines. The boundaries were imagined to be sub-grains. An electronmicrograph in Fig. 6 shows that minute slip lines at intervals of 500 Å. Orientation of this slip

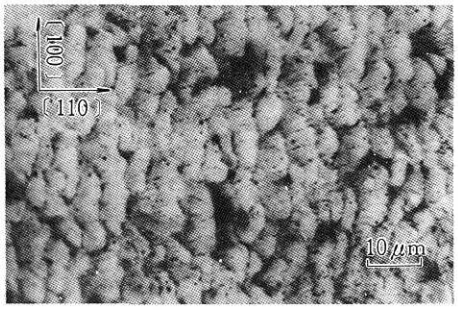

Fig. 5 Structure of fatigued surface on (1$\bar{1}$0) plane and [001] stress axis. Cottrell's sessil dislocation worked. $\varepsilon_a = 1.38 \times 10^{-3}$, $N = 1.5 \times 10^6$

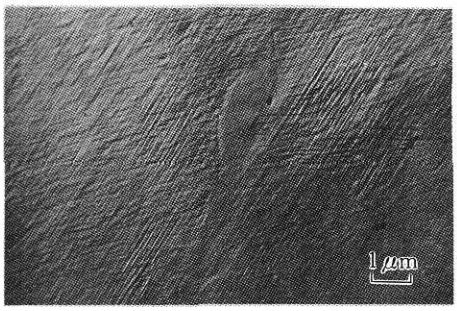

Fig. 6 Electron-micrograph of the same specimen as Fig. 5.

system was estimated as [112] or [11$\bar{2}$] and [110] for a crossing slip system. The angle had a deviation of about 5 degrees and the other slip lines had waviness. This was imagined to be originated from a strain inside the sub-grains, but a precise mechanisms were not clarified.

It was thought that the difficulty in forming cracks in this orientation would be originated from Cottrell's sessil dislocation in which the movement of dislocation was intercepted at the [001] axis. As shown in Fig. 7, the dislocations on the slip plane

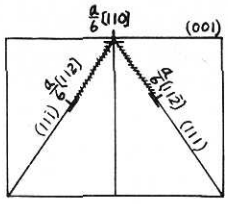

Fig. 7 Cottrell's sessil dislocation

(111) and (11$\bar{1}$) have Burgers vectors $\frac{a}{2}$[10$\bar{1}$] and $\frac{a}{2}$[011], respectively, and these were resolved in to directions as follows;

$$\frac{a}{2}[10\bar{1}] = \frac{a}{6}[2\bar{1}\bar{1}] + \frac{a}{6}[11\bar{2}]$$

$$\frac{a}{2}[011] = \frac{a}{6}[\bar{1}21] + \frac{a}{6}[112]$$

$\frac{a}{6}$[112] and $\frac{a}{6}$[11$\bar{2}$] lie on the specimen surface (110) and compose a dislocation $\frac{a}{6}$[110], which lies on [1$\bar{1}$0] and prevents slip. Because of these strong interactions, dislocation density was increased. Hardened cells were formed in which two parts with and without dislocation were divided. The former was composed of sub-grain boundaries which were pile-up of dislocations. In polycrystals, it was assumed that a crystal in accordance with these conditions could not be an origin of the cracks.

(3) **[112] stress axis**

Since the maximum Schmid factor was obtained along [011] orientation on (1$\bar{1}$1) plane and [101] orientatation on ($\bar{1}$11) plane, prominent slips and cracks appeared along [110] orientation which was a intersection of these surfaces and a single crystal surface. Since subsidiary slip orientations would be [01$\bar{1}$] and [10$\bar{1}$], a slip system along [11$\bar{2}$] could be formed, but this was very weak. Fig. 8 shows a

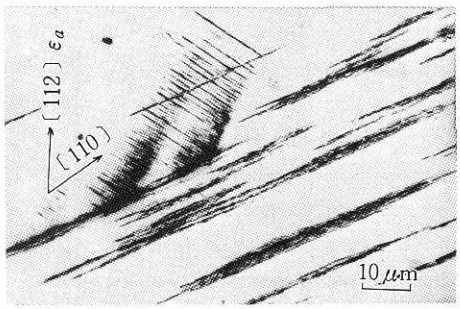

Fig. 8 Crack formation on (1$\bar{1}$0) plane and [112] stress axis.
$\varepsilon_a = 1.2 \times 10^{-3}$, $N = 1 \times 10^5$

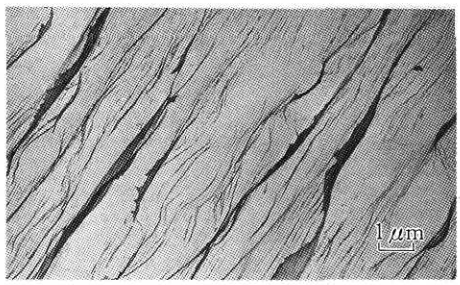

Fig. 9 Electron-micrograph of the same surface as Fig. 8.

photo-micrograph of these cracks and main slips appeared along [110] direction. Another slip system crossing at 26° with the main slips also appeared and the direction of the slip line crossed along a direction of bisecter of (112) and (110). Fig. 9 shows an electronmicrograph of these slip lines, waviness of these cracks would come from interaction of two slip systems.

(4) **[111] stress axis**

Six orientation in which Schmid factors are the same would contribute to crack formation. However,

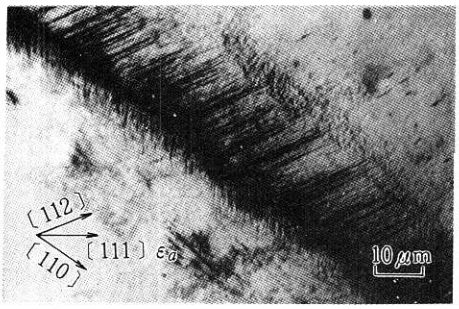

Fig. 10 Crack formation on $(1\bar{1}0)$ plane and [111] stress axis.
$\varepsilon_a = 1.2 \times 10^{-3}$, $N = 1 \times 10^5$

the slip planes were not symmetrical, but much complicated. Fig. 10 shows a photo-micrograph of the cracks. Broad and black line was along a [110] orientation. Its slip planes were $(1\bar{1}1)$ and $(\bar{1}11)$ and crossed with the specimen surface at an angle of 35° 16′. Fine cracks were linear and along [112] direction. Its slip plane $(11\bar{1})$ was vertical to the specimen surface. Out of three slip planes, [101] and [011] orientations are common in the specimen plane. Since [110] orientation became unbalanced by interaction of Burgers vector on $(1\bar{1}1)$ plane, the slip lines near the crack was wavy in shape. Fig. 11 shows an electron-micrograph of these slip lines. This also indicates that these were an initial stage

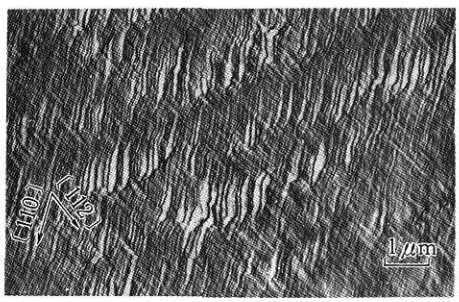

Fig. 11 Electron-micrograph of the same surface as Fig. 10.

of the crack formation, that the wavy lines were along [110], and that these had a certain cross angle with the specimen surface. Straight slip system had a cross angle with the former system at 54° 44′ and was along [112] orientations.

4. {111} surface

Table 2 Schmid factor of slip system on single crystal (111) surface

Cross line with (111) surface (Crack direction)	Slip system			Stress axis	
	Slip plane	Slip direction	No	$[10\bar{1}]$	$[11\bar{2}]$
	(111)	$[1\bar{1}0]$	1	0	0
		$[01\bar{1}]$	2	0	0
		$[10\bar{1}]$	3	0	0
$[\bar{1}10]$	$(11\bar{1})$	[101]	4	0	0.272
		$[1\bar{1}0]$	5	0.408	0
		[011]	6	0.408	0.272
$[\bar{1}01]$	$(1\bar{1}1)$	[110]	7	0	0.272
		$[10\bar{1}]$	8	0	0.408
		[011]	9	0	0.136
$[01\bar{1}]$	$(\bar{1}11)$	[101]	10	0	0.136
		$[01\bar{1}]$	11	0.408	0.408
		[110]	12	0.408	0.272

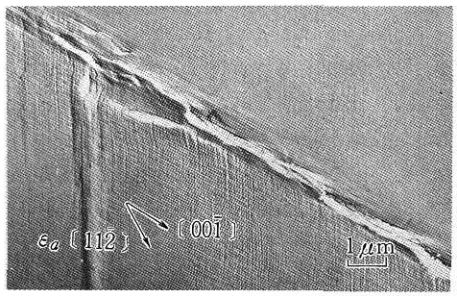

Fig. 12 Slip pattern and crack formation by fatigue test on (111) plane and $[11\bar{2}]$ stress axis.

Table. 2 shows the slip systems and values of Schmid facter for each stress axes. Fatigue tests were performed on $[10\bar{1}]$ and $[11\bar{2}]$ stress axes, and the result is shown in Fig. 12 for both cases, which shows slip lines and cracks cossing at 60° each other. For $[11\bar{2}]$ stress axis, these were formed on two orientations which have larger Schmid factors.

Acknowledgements

The authers would like to express their thanks to Professors H. Miyamoto and H. Kitagawa, University of Tokyo for their kind guidance and encouragement and to Professor Y. Ishida for his kind instruction.

(Manuscript received, August 3, 1977)

Reference

1) M. Matsunaga and Y. Hagiuda, This Journal, 25, 7, 300, 1973, and 25, 11, 491, 1973